

Carrier Sensing and Receiver Performance in Indoor IEEE 802.11b Mesh Networks

Abstract—In this paper, we address the following question: given a typical indoor IEEE 802.11 mesh network, how are carrier sensing, receiving and interference range related, and how stable are they in time? To answer this question, we conducted broadcast measurements in the Berlin RoofNet testbed under saturated conditions using multiple simultaneous transmitters with either carrier sensing turned on and off, respectively.

In contrast to several prior studies, our results indicate that wireless mesh networks are much more deterministic, and they show a high stability even under self-induced interference. Interestingly, for IEEE 802.11b at 1Mbps, the interference and carrier sensing range are only slightly larger and smaller compared to the receiving range, respectively. On the other hand, we identified uncontrolled external interference and environmental mobility as the key disturbing factors causing variations in packet reception and carrier sensing. In addition, the vendor specific estimation of Received Signal Strength Indication (RSSI) is vulnerable to interference on our Atheros hardware. Hence, RSSI estimates under interference should be handled with care.

I. INTRODUCTION

Nowadays, wireless mesh networks (WMNs) are a vital component of several applications. Starting from pure research objects, they are now operational access networks like community and campus networks, sensor networks or infrastructure networks in disaster recovery. One of the main success factors have been the broad availability of cheap hardware, the uncomplicated deployment and the robustness of such networks. Hence, this makes it even more astonishing that there is no consensus about fundamental properties of the network and its nodes. This paper presents a measurement study of the Berlin RoofNet, an indoor IEEE 802.11 WMN. In particular, we focus on the operation of IEEE 802.11b receivers and transmitters exposed to controlled and uncontrolled interference.

For IEEE 802.11b at 1 Mbps, our main results can be summarized as follows. The carrier sensing (CS) range is slightly smaller than the receiving range. In particular, we found that a packet success rate (PSR) around 10 % is a good indicator for CS. Furthermore, partial CS is seldom, although asymmetric CS is common and causes severe problems. Without interference, the receiver's Signal-To-Noise (SNR) to PSR curve is steep, i.e. the receiver performance matches the theoretical expectations from the AWGN channel. With controlled interference, the Signal-To-Interference (SIR) becomes the dominating measure for interference-limited links. With weak interference, the link remains noise-limited, and SNR dominates its performance. The interference range of a transmitter is only slightly larger than its receiving range. On the other hand, environmental mobility during daytime

and uncontrolled interference seriously disturbs the relation between PSR and SIR/SNR. Without both disturbing factors, links are surprisingly stable in time within minutes and hours. Furthermore, the hardware-estimated Received Signal Strength Indication (RSSI) has only a limited reliability, because interference causes multimodal RSSI distributions at the receiver, and the Atheros specific calibration invalidates the reported RSSI values.

II. RELATED WORK

Lots of measurements from IEEE 802.11 networks have been presented in the recent years. However, there is no generally accepted consensus about the origins of performance deficits of WMNs, the impact of interference, the accuracy of CS and the reliability of RSSI estimates.

For example, Aguayo et al. present results from an outdoor IEEE 802.11 network [1]. They observe that intermediate loss rates are common, and that SNR has little predictive value for PSR. They argue that multi-path fading contributes the most to the observations, and external interference is negligible. In contrast, other studies [2], [3] suggest that signal strength is a reliable predictor for PSR, and in particular, interference distorts this relationship. Furthermore, Zhang et al. propose a SNR-guided bit-rate adaptation algorithm [4] based on measurements with IEEE 802.11a. From their measurements, they conclude that the PSR transition zone is small and hardware dependent without interference. On the other hand, Bicket et al. do not find the SNR-PSR relationship useful in rate adaptation [5].

Other studies aim at characterizing the interference relation within the network. For example, Padhye et al. develop a model, which predicts conflicts from a limited set of measurements [6]. However, the model operates at the logical link level and does not allow further insight in the operation of the physical link. A further study by Das et al. investigates multi-way interference [7]. They conclude that multi-way interference, although it may have significant impact, is not widespread in typical IEEE 802.11 networks.

Besides the above-mentioned network-centric investigations, several studies focus on the operation of individual links. For example, Lee et al. have conducted several measurements on the interference and CS relation for indoor 802.11a networks. In [8], they observed that asymmetric CS and/or interference relations commonly exist, i.e. CS works in one direction only. They characterized the throughput and goodput for two links systematically for several categories of CS and interference. In particular, one-way hidden interference and

mutual interference & asymmetric CS results in unfair unicast throughput, and links in the mutually hidden interference category both suffer from poor performance.

In addition, Lee et al. [9] characterized the receiver performance in the presence of interference, which indicates that Atheros hardware implements the Message-In-Message physical capture method. Furthermore, they observed that there could be gray zone of 3 dB in which CS and interference apply partially [10]. They propose to represent CS and interference by continuous values to capture the gray zone. In [11], they propose a model, which predicts the relation of CS and interference based on signal power. Interestingly, Kai et al. also observed partial CS [12]. However, they estimated CS in relation to distance instead of SNR; hence, the validation of the results is hardly possible. Furthermore, both authors have not discussed how the two-level CS in IEEE 802.11a contributes to partial CS. Remember that mode 3 CCA consisting of preamble and energy detection is mandatory in IEEE 802.11a/g.

III. MEASUREMENT SETUP AND METHOD

We conducted measurements in an indoor IEEE 802.11 WMN located in the main building of the Computer Science Department at Humboldt University Berlin. It is a multi story building mostly consisting of concrete, steel, glass and dry walls. In particular, we used 14 Netgear WGT634U routers, which are equipped with an IEEE 802.11bg compliant WiFi card from Atheros.

A single measurement trial consisted of two types of experiments. At first, a single sender was transmitting UDP packets with 1460 Byte payload at 1 Mbps for 30 seconds. In order to saturate the wireless medium, we fixed the TXR at 80 packets per second. The remaining nodes recorded all packets received from the transmitter along with the reported RSSI. Due to our experiences with RSSI (see section IX), we use the terms RSSI and effective RSSI instead of SNR and SIR throughout the paper. We repeated the experiments until each node has once been the transmitter.

Afterwards, we added another, operational equal transmitter, and repeated this type of experiment for all possible transmitter pairs. In sum, the 14 and 91 experiments with 1 and 2 transmitters, respectively, took about 3 hours, because we re-initialized the nodes after each experiment. This way, we were able to conduct four measurement trials during a night from 8 pm to 8 am. Table I summarizes the parameters settings for all measurement trials. In particular, we varied the RF channel (Ch.), the transmission power (Pw.), the processing of CRC corrupted frames, whether the channel clear assessment (CCA) and calibration (Calib.) was activated, and whether the measurements took place at a weekend (WE) or during daytime (DT). In the following, for each transmitter and receiver combination we use the term primary link for the considered link from source to destination, and secondary link denotes the link from an interferer to the destination.

During the experiments, we turned off all Atheros proprietary features. This applied in particular to the Ambient Noise

Version	Ch.	Pw.	CRC	DT/WE	CCA	Calib.
1.34 - 1.37	14	20	✓	- / -	✓	✓
1.41 - 1.44	14	10	✓	- / ✓	✓	✓
1.45 - 1.48	14	1	✓	-✓/ ✓	✓	✓
1.49 - 1.52	14	15	✓	- / ✓	✓	✓
1.57 - 1.59	14	20	✓	✓/ -	✓	✓
1.60 - 1.62	6	20	✓	- / -	✓	✓
1.63 - 1.65	6	20	✓	✓/ -	✓	✓
2.10 - 2.13	14	20	✓	- / -	-	-
1.66 - 1.69	14	20	-	- / -	✓	-

TABLE I
MEASUREMENT PARAMETERS

Immunity and diversity. Unless stated otherwise, the driver processed packets with CRC and PHY errors and regularly calibrated the hardware. We used the IEEE 802.11 channels 6 and 14. Among others, the wireless campus network heavily uses the former channel, whereas the latter is free due to regulations of spectrum usage in Germany. However, we experienced co-channel interference from devices operating at adjacent RF channels. In order to increase the number of covered scenarios, we performed measurement trials at 4 different power levels. Furthermore, the driver provides a continuous transmit mode, in which the device does not perform CS and transmits even in the presence of a transmitting neighbor. In order to analyze the receiver performance in isolation we performed measurement trials with CS turned off at the transmitters. However, we only disabled virtual and physical CS in the modified driver¹. Using the additional modes with shorter inter-frame spacing and modified queue processing, the neighbors hardly received any packets. Nevertheless, with CS turned off, even links having an RSSI above 50 dB exhibit PERs of at least 6 %. Furthermore, the losses had a high correlation across receivers; hence, we argue that the transmitter is the problem.

IV. RECEIVER PERFORMANCE WITHOUT INTERFERENCE

As lined out in [5], theoretic results from the AWGN channel suggest that the transition zone from high to low PSRs is small in terms of SNR. Fig. 1a shows PSR versus RSSI from our experiments on channel 14 with only a single transmitter. Every point represents the RSSI and PSR of an individual experiment, averaged over the measurement duration of 30 sec. Although we transmitted frames larger than 1500 Byte, the graph presents the receiver performance for small packets, since we have processed corrupted packets down to a minimal length of about 50 Byte. Interestingly, the results from experiments without corrupted packets are not significantly different.

Certain nodes like node 81 and 41 exhibit an exceptional high packet loss for links with an RSSI above 10 dB. The curves for both nodes are depicted in Fig. 1b in isolation. On both nodes, we have seen traffic from other sources like the wireless campus network even on channel 14. We suppose that these nodes are seriously affected by co-channel interference generated by nearby nodes. Thus, we consider this

¹<https://systems.cs.colorado.edu/projects/carp>

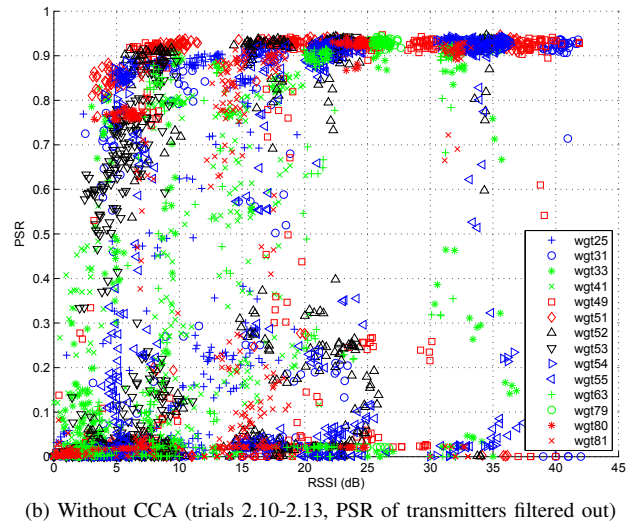
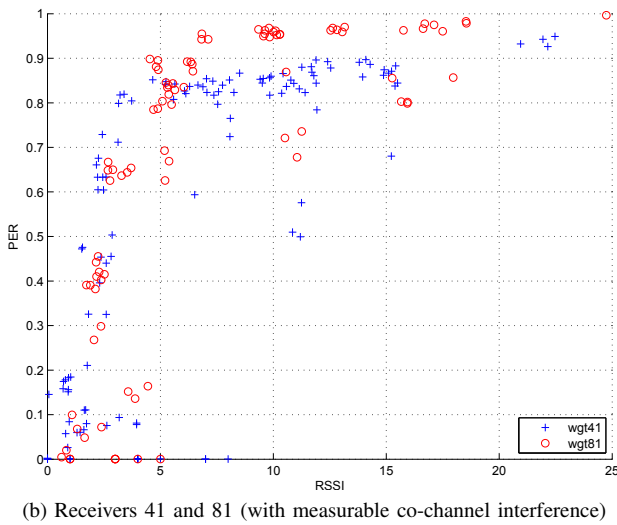
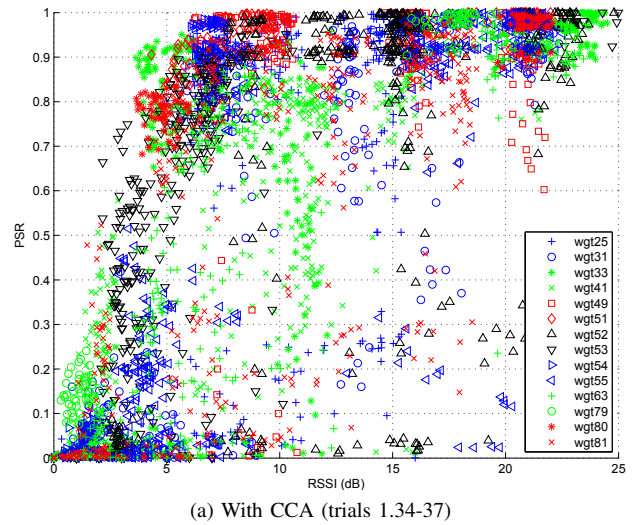
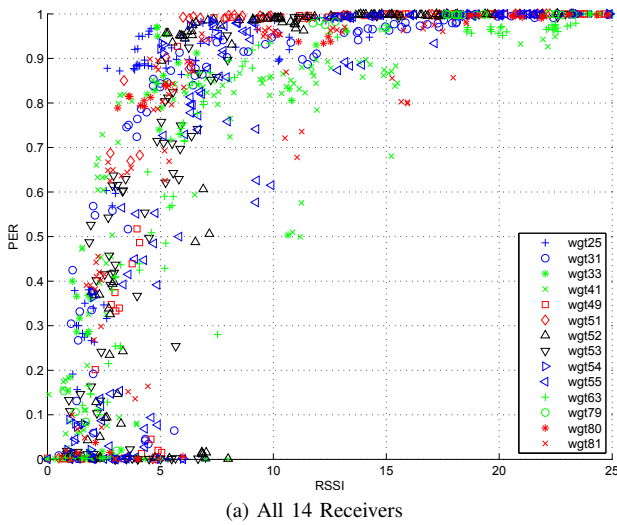


Fig. 1. PSR versus RSSI for the experiments with a single transmitter on channel 14 (trials 1.34-1.52).

Fig. 2. PSR versus RSSI for the experiments with two transmitters on channel 14.

behavior exceptional and focus on the remaining results in the following. The same applies to data points with very low PSR, since the statistical confidence of these points is low.

On these premises, a significant decrease in PSR starts at 8 dB and ends at 4 dB, i.e. for a PSR of 90 % the RSSI has to be above 4 dB. For a PSR level of 10 %, the RSSI ranges from 1 dB to 6 dB, although the majority of links fall within 1 to 4 dB. Furthermore, the diagram shows that RSSI values are hardly comparable across receivers. For example, node 63 reaches the 90 % PSR level at 8 dB, whereas node 25 hits this level at 4 dB RSSI. In summary, the receiver performance in terms of PSR and RSSI matches the theoretical results closely for our experiments during nighttime and without interference. There is a small transition zone of up to 7 dB, in which the PSR goes from one to zero. However, the localization of this zone may vary across receivers.

The results change if there are two active transmitters during an experiment. As shown in Fig. 2a, the additional interference

distorts the sharp PSR-RSSI relationship. An RSSI of 15 dB is no longer a guarantee for high PSRs. High packet losses still occur for RSSI values of up to 28 dB. On the other hand, the nodes 51, 54, 79 and 80 are less affected by interference. They lose only about 10 % PSR at maximum, which may be due to missing hidden nodes and CSMA inherent collisions only. When switching off the wireless cards CCA (Fig. 2b), high packet losses occur for all links, with those with very high RSSI values of up to 70 dB. The results clearly show that RSSI as reported by Atheros cards is not able to capture interference during frame reception. Furthermore, IEEE 802.11 compliant interference distorts the PSR-RSSI relationship for links below 25 dB RSSI, and non-compliant interference renders the PSR-RSSI relationship meaningless without further information about the sources of interference.

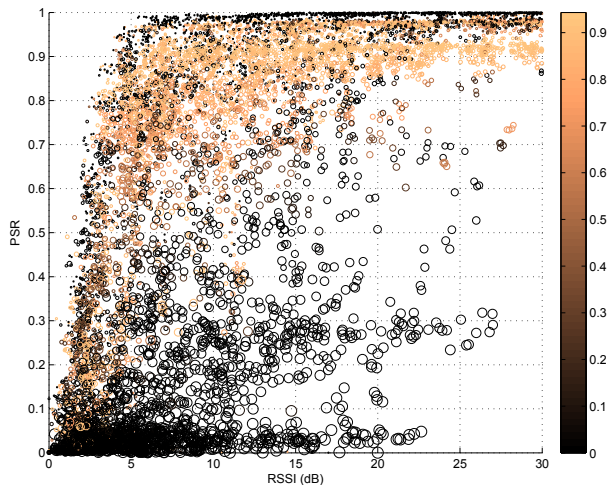


Fig. 3. PSR versus RSSI for the experiments with two transmitters on channel 14 (trials 1.34-1.52). The size of the markers (area) corresponds to the absolute loss in PSR due to interference, i.e. the loss for the point at 20 dB RSSI and a PSR close to 0 is almost 1. The marker color indicates the PSR on the inter-transmitter link.

V. RECEIVER PERFORMANCE WITHOUT CARRIER SENSING

In order to characterize the receiver further, we analyze the PSR-RSSI relationship depending on the absolute loss in PSR due to interference. We define the PSR loss as the difference in PSR of the interference-free and the interfered link. Note that both values are determined in individual experiments, which are separated in time by some minutes. Although links may vary over time, the PSR loss is a meaningful measure, as we will illustrate in section VIII.

Fig. 3 shows the PSR loss ranging from 0 to 1 as size of the markers. Furthermore, we colored the data points according to the PSR of the inter-transmitter link. The lighter shaded data points indicate better links between both transmitters. The CSMA inherent collisions cause packet loss in the range of 4 - 10 %, which also apply to high SNR links with an RSSI of up to 85 dB. On the other hand, for data points with high PSR loss, the quality of the link from transmitter to interferer is generally low, which suggests that the hidden node problem dominates on these links. However, considering only the transmitter-interferer link is not sufficient. For example, at the upper border of the diagram, there are many links without a significant loss in PSR although the link to the interferer is weak.

For links, which are weak even without interference, the above-introduced measure of absolute PSR loss does not capture the impact of additional interference-caused packet loss. For example, an absolute PSR loss of 30 % is more severe on links with interference-free PSR of 40 % compared to an almost loss-less link. Hence, we define the relative remaining PSR as ratio of interference-affected to interference-free PSR. Furthermore, the relative PSR loss is defined as difference of relative remaining PSR to 1. For the experiments on channel 14 without CCA, Fig. 4a and Fig. 4b illustrate both measures

as marker diameter in relation to the strength of both primary and secondary link. Note that both diagrams contain the same data points. They differ only in the size of the markers for illustration purposes. The marker color corresponds to the relative PSR loss in both cases. Furthermore, the diagrams are symmetric with respect to the diagonal of the coordinate system, and they contain 3861 data points each.

In the diagrams, we identified four operational areas. Along the diagonal band for which the strength of the primary link $RSSI_p$ is slightly higher than the strength of the secondary link ($RSSI_s$), there is a transition region with intermediate PSR loss rates. Note that the transition zone is not centered at the diagonal of the diagram; instead, it is shifted to the right by some decibel. In the triangle above the diagonal band, the secondary link is stronger and causes total loss on the primary link. In the triangle below the transition zone, the communication remains unaffected. However, the transition zone seems to become broader for weak links between 0 dB and 10 dB. However, the statistical confidence of data points in either of the two low RSSI areas is lower, because of the smaller number of arrived packets, which even decreases to total loss under interference in some cases. Hence, in Fig. 4c and Fig. 4d we replaced the actual RSSI of all links by those values obtained in interference-free (single-sender) experiments. In the resulting diagrams, the transition band is not linear any more in both RSSI values. The linear extension of the band would cut the abscissa at about 10 dB. Instead, there are many weak links between 4 dB and 10 dB, which are able to communicate with high remaining PSR despite interference of up to 4 dB. The results indicate that other effects like noise begin to play a role in the considered RSSI range.

The effective RSSI ($RSSI_e$) is the difference of $RSSI_p$ and $RSSI_s$. It corresponds to the SIR if the RSSI is interpreted as SNR. Fig. 5 shows the effective RSSI in relation to the resulting PSR. We neglected the tails on both sides, since they continue at a high and low level, respectively, without significant changes. In contrast to Fig. 2b, which shows $RSSI_p$ in isolation, now there is a transition zone from high to low PSR of about 20 dB. Furthermore, the receiver performance depends on the absolute strength of the link, as indicated by the different colors. Weak links of up to 7 dB, which are shaded dark, have a rather steep transition comparable to Fig. 1a. There are some outliers to the left, for which the reason is most likely the missing noise component within $RSSI_e$. Interestingly, for stronger links above 7 dB and 14 dB the transition becomes less steep. Lee et al. showed that the receiver performance in the interference-limited regime differs from the noise-limited regime [9], [11]. They identified two distinct performance characteristics in the case of physical capture, depending on which frame arrives first at the receiver. However, as our results indicate, a mixture of both cases most likely affects typical indoor WMN. Hence, the canonical results in [9], [11] are the extreme cases for the receiver performance in WMNs. However, we leave further investigations in relation to the overlapping of arriving frames

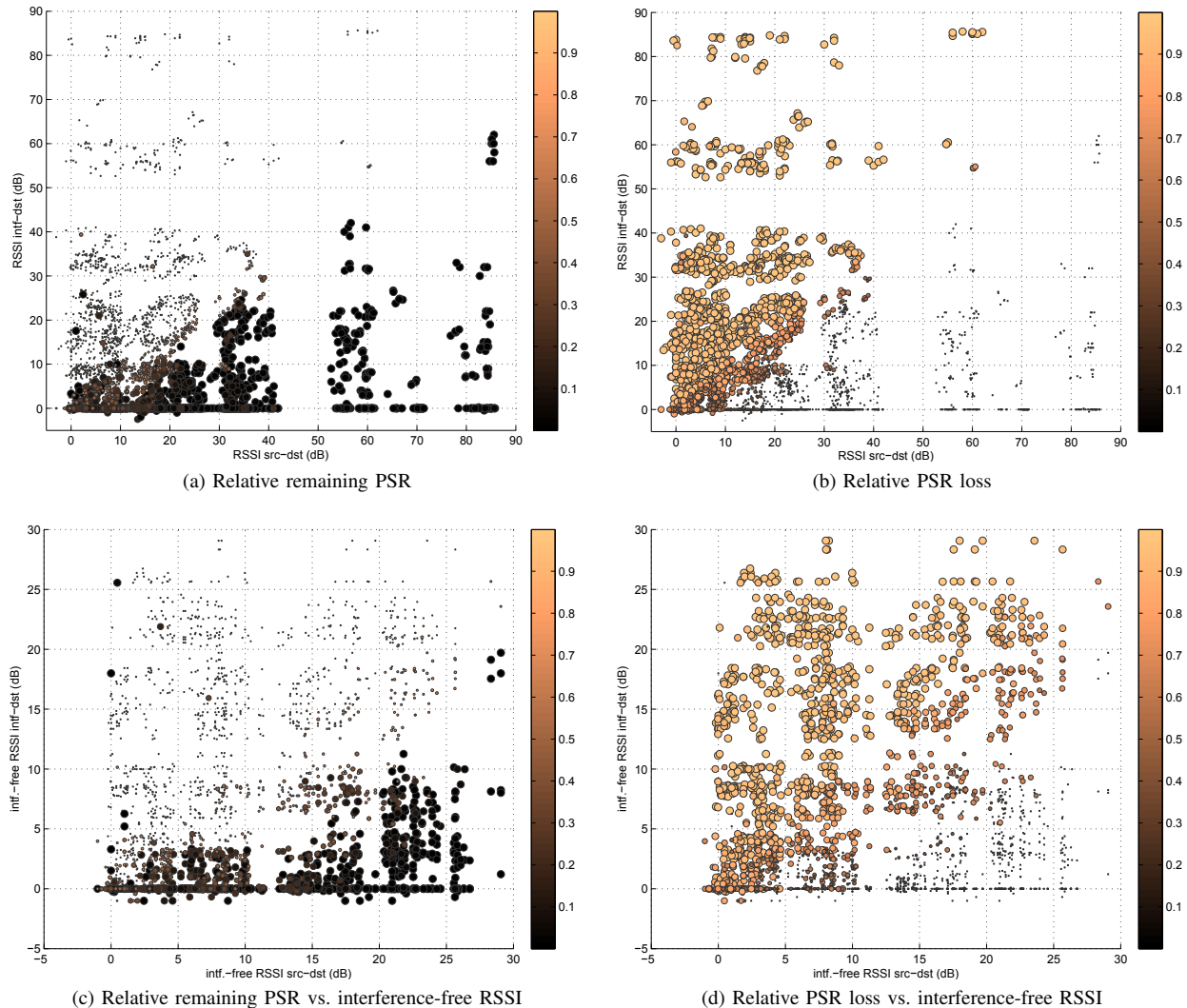


Fig. 4. Relative remaining PSR and PSR loss due to interference (marker diameter and color) in relation to the RSSI of the primary (src-dst) and secondary (intf-dst) link, respectively, for the experiments with two transmitters on channel 14 and disabled CCA (trials 2.10-2.13). The latter two diagrams differ from the former in that the RSSI of each link stems from interference-free (single-sender) experiments. Missing RSSI values are set to 0, and the inter-transmitter links are filtered out.

for future work.

In addition, we are interested in determining the interference range of a transmitter. In Fig. 6, we generated a CDF of absolute and relative PSR loss over all available links (4742 values) and over weak secondary links only (1996 values). Note that the latter is a subset of the former set of all links, and the criterion $PSR_i < 1\%$ on the secondary link includes all cases in which there is virtually no secondary link. We used the interference-free secondary PSR because the missing CCA favors stronger primary links. The relatively low number of weak secondary links indicates that our network is dense.

In about 40 % (25 %) of all possible combinations of source, destination and interferer, the relative (absolute) loss in PSR is more than 50 %. The diagram shows that PSR losses affect the group of weak secondary links under-proportionally. In particular, only 5 % of all weak secondary links cause an absolute PSR loss of more than 0.1. On the other hand, these

5 % contribute to relative PSR losses of 0.66 and above, indicating that especially weak primary links are affected. In summary, stronger secondary links cause the majority of serious PSR losses. Hence, it is unlikely that a transmitter causes serious losses and the receiver is not able to see the hidden node. In other words, the interfering range of a transmitter is only slightly larger compared to its receiving range. Referring back to Fig. 1a, this result is not surprising, since the gap between receiver sensitivity and the noise floor is small. Note that the results apply to a bit rate of 1 Mbps, and further investigations with other bit rates are left for future work.

VI. PERFORMANCE OF CARRIER SENSING

The IEEE 802.11b standard proposes three CS modes, which consist of signal detection, energy above threshold and a combination of both [13]. Note that for the OFDM

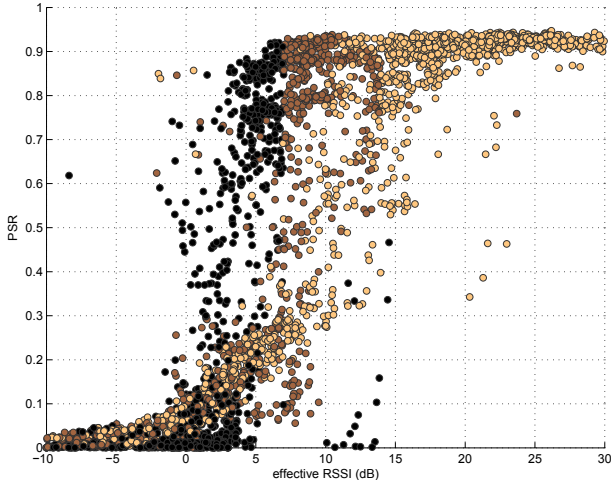


Fig. 5. PSR versus effective RSSI for the experiments with two transmitters on channel 14 and CCA turned off (trial 2.10-2.14). Each of the tree color shades corresponds to an RSSI range for the primary link: RSSI values up to 7 dB are shaded dark, values between 7 dB and 14 dB are shown slightly lighter, and the lightest shade is used for links above 14 dB. Missing $RSSI_s$ values are set to 0, and inter-transmitter links are filtered out.

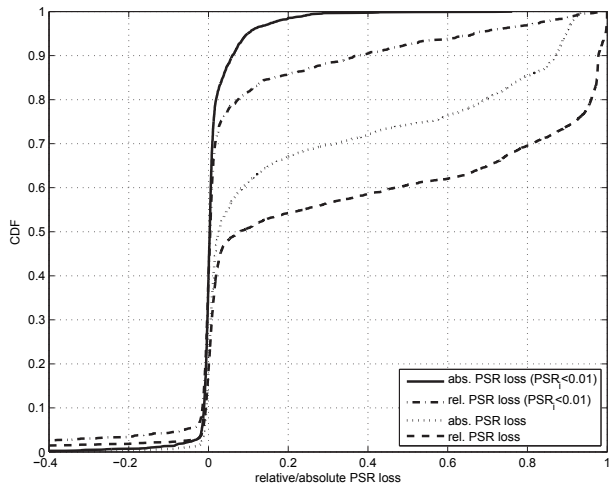
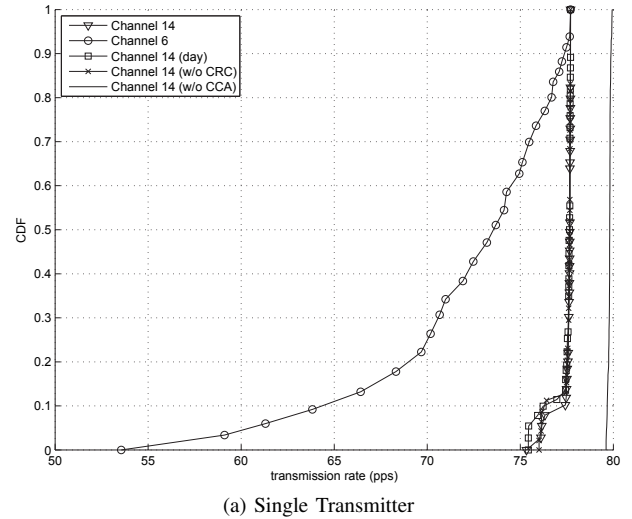


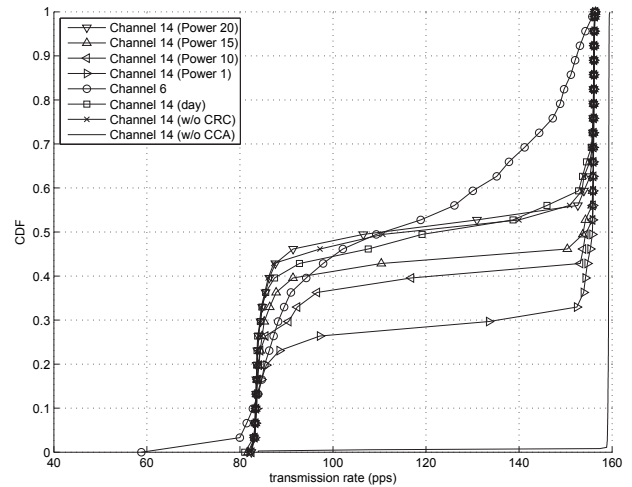
Fig. 6. CDF of relative and absolute PSR losses for all links (4742 values) and links with inference-free $PSR_f < 0.01$ (1996 values), respectively, for trials 2.10-2.14 (two transmitters, channel 14, CCA turned off). Data points for links between two simultaneously active transmitters are filtered out.

physical layers in IEEE 802.11a/g, the combined mode became mandatory [14], [15].

For our test-bed nodes, we have validated that all of them are able to achieve the maximum TXR when CCA is turned off. In particular, the TXR are between 79.25 packets per second (PPS) and 79.95 PPS for all 784 transmitters of trials 2.10-2.13 with only 3 outliers. When turning on the CCA, the maximum TXR is slightly lower (see Fig. 7a). Furthermore, in 10 % of all cases this maximum is not achieved, which indicates that co-channel interference is present. In contrast, on channel 6 only few nodes achieve the maximum TXR even at night. In particular, in 25 % of all cases the TXR is below 70 PPS. If we assume that only few people have been present



(a) Single Transmitter



(b) Two Transmitters

Fig. 7. CDF of sum TXR per experiment. The category “Channel 14” consist of four transmission power levels (trials 1.34-1.52). Since there are no significant differences between them, they are grouped in the upper diagram. The remaining categories belong to the trials 1.60-1.66, 1.57-59, 1.66-1.69, and 2.10-2.13 respectively.

during these nightly experiments, the high costs of beaconing become obvious.

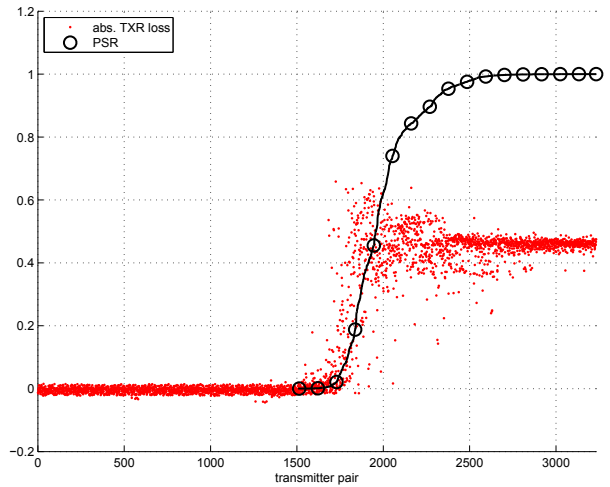
In the experiments with two transmitters, we summed up the TXRs of both transmitters in Fig. 7b, because the individual rates are unfair in some cases. The diagram indicates that CS works well on the interference-free channel 14. The transition region from perfect sensing to no sensing is steep for all four power levels, i.e. only few transmitter pairs experience partial CS. During daytime, the transition region is slightly shallower. On the other hand, the transition zone is shallow on channel 6. In particular, about 23 % of all transmitter pairs achieve a cumulated TXR between 100 PPS and 140 PPS, whereas this region only contains 4-6 % of the transmitter pairs on channel 14. However, from the single sender experiments, we are aware that this channel is RF polluted; hence, reasoning about partial CS on channel 6 is not possible.

In the next step, we are investigating the CS range in

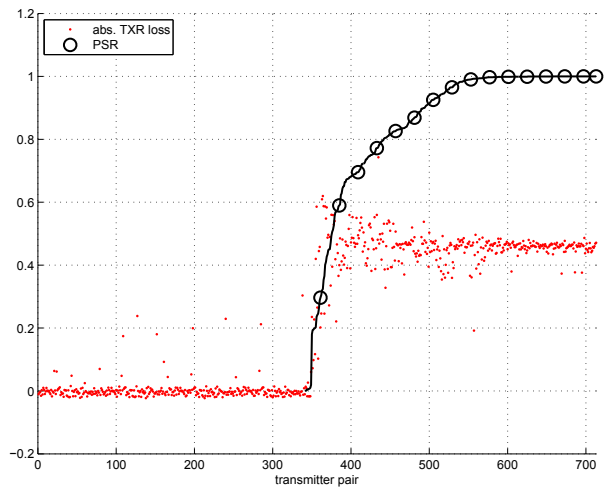
relation to the receiving range. In order to assess the effect of CS, we introduce an indicator named relative TXR loss. The relative TXR loss is defined as the absolute TXR loss due to interference, i.e. the difference of interference-free TXR and TXR under interference, relative to the interference-free TXR. Note that both values originate from different experiments separated in time by some minutes. Nevertheless, we will point out that this measure is meaningful in section VIII. The relative TXR loss for all transmitter pairs on channel 14 with processing of CRC corrupted packets is depicted in Fig. 8a in relation to the PSR of the link in-between. The diagram shows that the relative TXR loss is negligible for transmitter pairs, which are not able to exchange packets, i.e. the CS range is smaller than the receiving range. Furthermore, most TXR losses are small for PSR's below 5-10 %. In contrast, for high PSR links the TXR losses are in the order of 0.5, i.e. both nodes share the medium in a fair way. In-between low and high PSR links, there is a range of varying TXR losses originating mostly from unfairness in sharing of the wireless medium. We suppose that the EIFS processing is one source of unfairness as pointed out in [8]. However, a detailed investigation of this matter is left for future work. When turning off the processing of CRC corrupted packets, however, transmitter pairs with significant TXR losses and without packet delivery appear. Nevertheless, all other observations apply to these results, as well.

Now, the question arises how much smaller the CS range is in relation to the receiving range. Fig. 9a shows the relative TXR loss in relation to the quality of the inter-transmitter link in both forward (src-intf) and backward (intf-src) direction. In addition, the color of the markers indicates the TXR difference of both transmitters, which is a measure for the fairness in medium access. Furthermore, the relative TXRs, which are above 0.5, are shown in Fig. 9b in the same way. Note that both diagrams are symmetric with respect to the diagonal when ignoring the marker size. Above a PSR of 20 % in both directions, the TXR loss is in a range between 0.3 and 0.6, hence CS works well. However, asymmetric inter-transmitter links appear beside the diagonal and exhibit TXR losses, which are slightly away from the expected loss of 0.5. Above the diagonal, the inter-transmitter link is stronger in the forward direction from source to interferer, and it experiences higher TXR losses. The TXR difference is significantly below zero in the range from -0.2 to -0.1, i.e. the interferer increases its TXR at the expense of the source node. Due to the symmetry of the diagram, the opposite can be observed below the diagonal. We suppose that the EIFS processing causes the unfairness in the medium access. However, this issue needs further investigation.

In Fig. 9a, if the inter-transmitter links is weak in the forward direction, e.g. exhibiting a PSR below 10 %, the source experiences serious TXR losses in combination with high negative TXR differences. When reversing the roles of source and interferer, we see in Fig. 9b that the former interferer achieves a significantly higher TXR. Putting both observations together, we argue that CS works only in one direction of the



(a) With CRC/PHY errors (trials 1.34-1.57)



(b) Without CRC/PHY errors (trials 1.66-1.69)

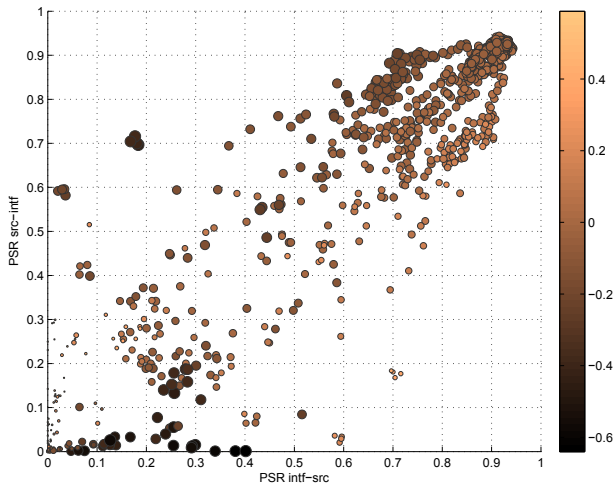
Fig. 8. Relative TXR loss for all transmitter pairs, ordered according to ascending (interference-free) PSR, on channel 14 with and without processing of CRC/PHY corrupted frames. Missing PSR values indicate that no communication is possible.

inter-transmitter link, i.e. it is highly asymmetric. Furthermore, we observed that unfairness and asymmetric CS is common. As shown in Fig. 10, about 25 % (10 %) have an absolute TXR difference of higher than 0.1 (0.2).

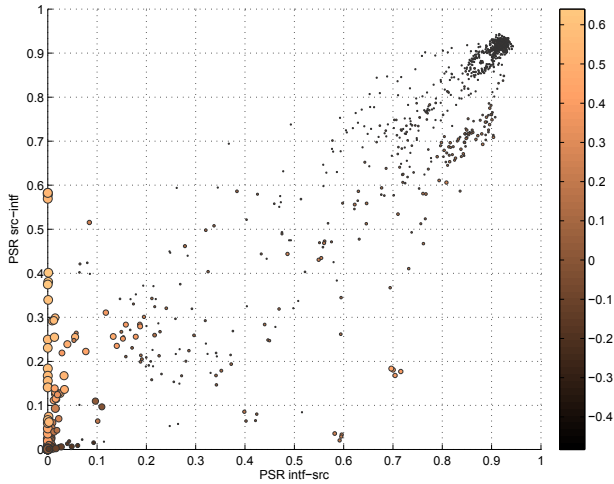
We have not found the RSSI useful for estimating the relative TXR loss. For strong links above 5-6 dB, there is a clear trend for fair medium sharing. Weak links, on the other hand, vary arbitrary between no transmitter conflicts, perfect CS and unfairness.

VII. RECEIVER PERFORMANCE WITH CARRIER SENSING

Depending on whether two transmitters can carrier-sense each other, the resulting receiver performance differs. We empirically determined a PSR value of 10 % as discriminator for CS. Nevertheless, other classifications are also possible. For example, using 20 % relative TXR loss produces a comparable good classification.



(a) Relative TXR loss. High PSRs in both directions of the inter-transmitter link result in a fair medium share with a relative TXR loss of 0.5



(b) Relative TXR above 0.5

Fig. 9. Relative TXR loss and relative TXR at the source (marker diameter), respectively, in relation to the PSR of the inter-transmitter link in both forward and backward direction (trials 1.34-1.52). The marker color indicates the TXR difference between both directions. Positive TXR differences (lighter shaded) indicate higher TXRs at the source. A fair medium share with equal TXRs results in a difference of zero, and higher TXRs at the interferer are shaded dark (negative TXR difference).

In Fig. 11, we plotted PSR versus effective RSSI (SIR) for inter-transmitter links having a PSR of 10 % and below. As expected, the diagram is similar to the corresponding curve without CS in Fig. 5. However, there are some outliers. As in the former graph without CCA, some links show intermediate PSRs for an RSSI between -20 dB to 0 dB. Again, we suppose that the most likely reason is the missing noise component within the effective RSSI. On the other hand, there are some outliers with negative effective RSSI, which typically have a PSR below 0.25. The results indicate that our CS discriminator is not perfect; nevertheless, it categorizes the CS relationship reasonable well.

For all inter-transmitter links above the PSR threshold of

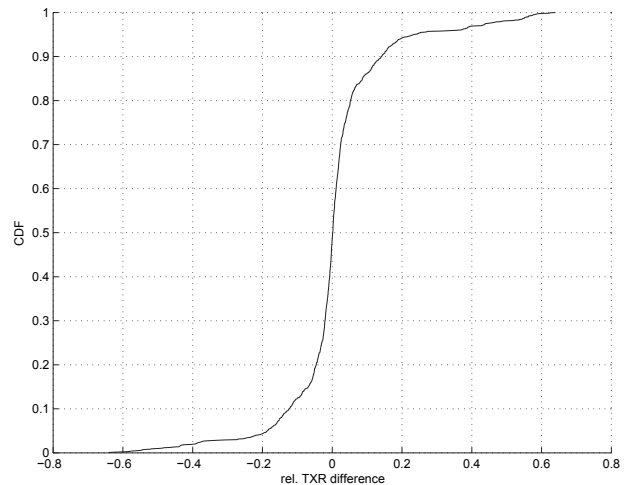


Fig. 10. CDF of the difference in relative TXR between both transmitters (trials 1.34-1.52).

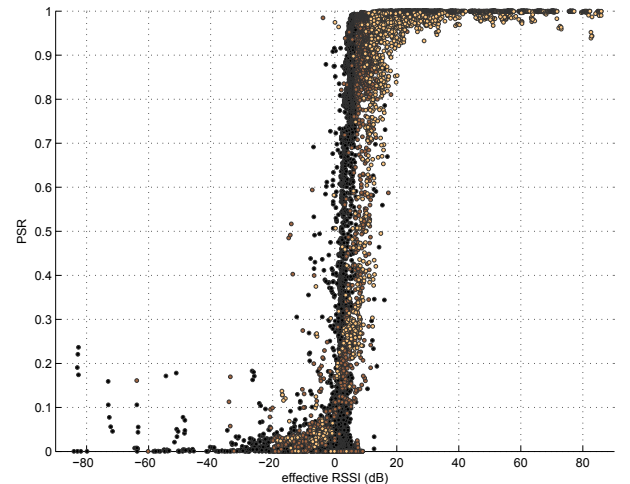
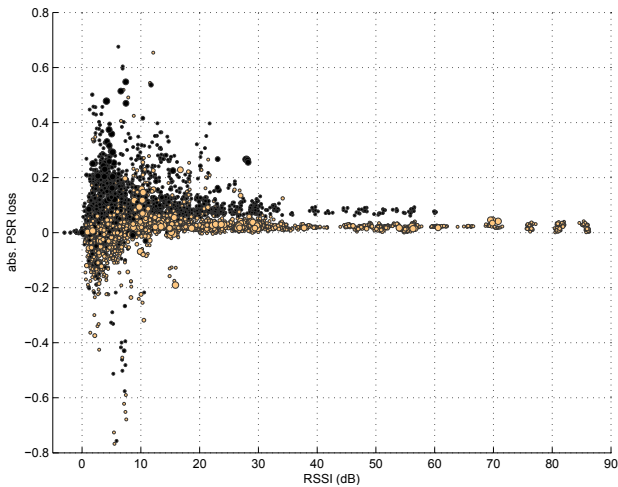


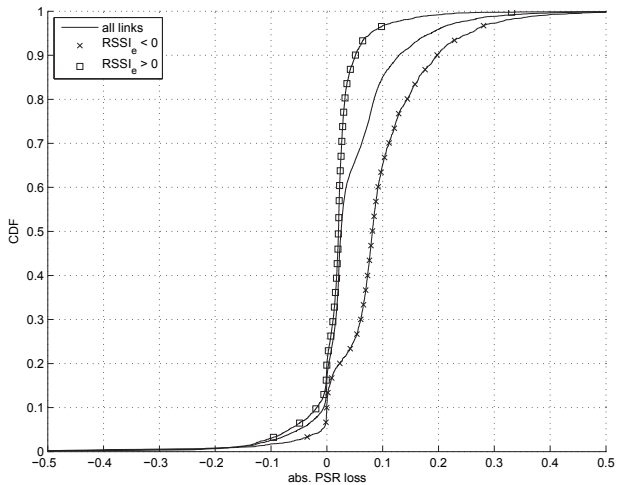
Fig. 11. PSR vs. effective RSSI (SIR) for inter-transmitter links having PSR < 0.1 in both directions (trials 1.34-1.52). Thus, CS is limited between both transmitters. The marker colors indicate an RSSI at the receiver below 7 dB, 7 dB to 14 dB, and above 14 dB, respectively, in the order from dark to light shades. Inter-transmitter links are filtered out.

0.1, we plotted the PSR loss due to interference versus the RSSI of the primary link in Fig. 12a. The color of the markers indicates whether the primary or the secondary link is stronger at the receiver. Most of the PSR losses are below 0.05 if the primary link is stronger. In particular, the CDF in Fig. 12b shows that the PSR loss is higher than 0.1 (0.05) in only 2.5 % (10.5 %) of all cases. On the other hand, there is no systematic reason why interference should cause negative PSR losses, i.e. the link quality improves with interference. We attribute negative PSR losses to measurement errors and link changes. Remember that the estimation of the PSR loss involves two measurements, which are spaced in time by some minutes.

If the secondary link is stronger than the primary one, the PSR loss is generally higher. For example, the median loss in Fig. 12b is 0.08 in the former and 0.02 in the latter case. We suppose that the CSMA inherent collisions are the



(a) PSR loss vs. RSSI for the primary link. The dark and light shades represent effective RSSI values below and above zero, respectively. Data points with unfair TXRs between transmitter and interferer are shown with larger markers.



(b) PSR loss CDF for all links and divided according to positive and negative effective RSSI.

Fig. 12. Loss in PSR due to two active transmitters for inter-transmitter links having PSR > 0.1 in both directions (trials 1.34-1.52). Generally, CS works well between both transmitters. Inter-transmitter links are filtered out.

main reason for the results. According to IEEE 802.11, each node with packets to send starts a random backoff after the medium becomes idle. If the backoff timer exceeds and the medium has been idle in the meantime, the node starts to transmit. The backoff duration is measured in terms of slot durations, which are multiplied by a discrete random number between 0 and 32 in IEEE 802.11b. Hence, according to [16] the CSMA inherent collision probability is 0.0625. This way, the transmitters overload the medium as shown in Fig. 7b. Whereas the TXR of a single sender is around 77 PPS, the sum TXR of two senders is about 83 PPS.

If the primary link is stronger, the physical layer capture effect prevents from these losses. In contrast, with stronger secondary links, the collisions result in packet loss. Nevertheless, the CDF in Fig. 12b shows that the significant amount

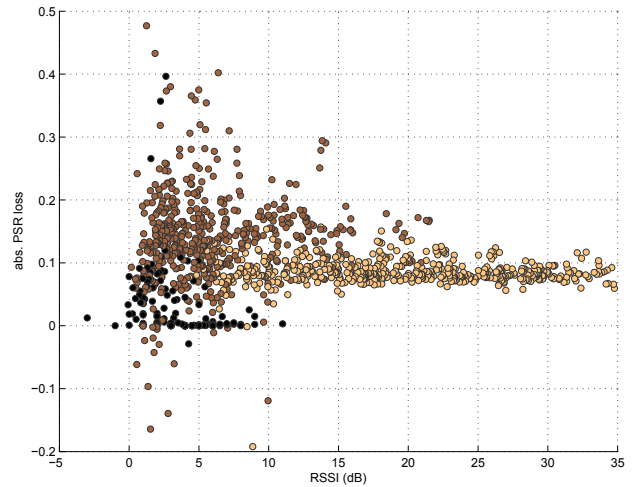


Fig. 13. PSR loss vs. RSSI for inter-transmitter links only (trials 1.34-1.52). If the PSR is above 0.8 (below 0.1) in both directions, the marker is shaded lighter (darker). Five outliers above 0.5 or below -0.2 are clipped.

of 25 % of these links show PSR losses between 0.1 and 0.2, and 10 % show even higher losses. Some of the higher losses above 0.2 occur in combination with an unfair TXR distribution between both senders, as indicated by the larger markers in Fig. 12a. We noticed that one particular reason is imperfect CS. For example, if one sender transmits not only the expected 40 PPS but also 10 % in addition, and it has the weaker link to the destination, it will experience higher packet losses. Fig. 13 illustrates the PSR loss on the inter-transmitter links. It is evident that especially the intermediate quality links with a PSR between 0.1 and 0.8 contribute to higher PSR losses. However, a detailed evaluation is left for future work.

For the sake of completeness, we present the CDF of absolute and relative PSR losses with CCA turned on in Fig. 14. Due to reduced transmission power, the fraction of weak links increases compared to our experiments without CCA in Fig. 6, i.e. the density of the network is lower. Considering the absolute PSR loss in all cases, the situation improves: The number of nodes with losses above 0.30 reduces from 30 % to 10 % due to CCA and the less dense network. On the other hand, the CDF for weak secondary links does not change significantly. Hence, the experiments support our assumption from above: The interfering range of a transmitter is only slightly larger compared to its receiving range.

VIII. LINK STABILITY UNDER UNCONTROLLED INTERFERENCE AND ENVIRONMENTAL MOBILITY

In the first place, our evaluation crucially depends on stable packet delivery and stable TXRs, since we have compared results from different experiments. However, this characterization may also be valuable for the operation of a WMN. For example, the estimation of the ETX metric [17] relies on the assumption that packet delivery is stable over intervals of some seconds.

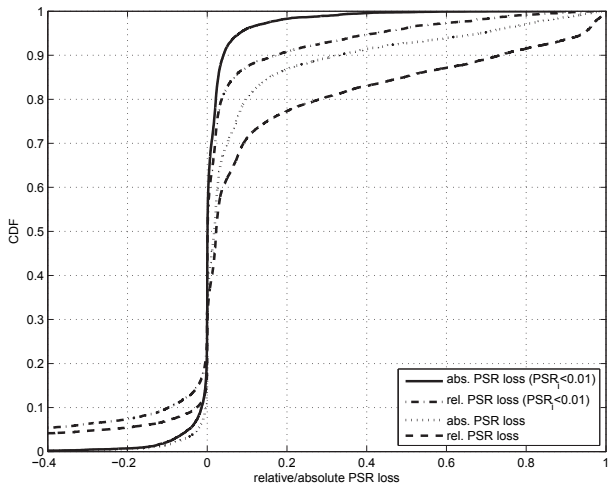


Fig. 14. CDF of relative and absolute PSR losses for all links (15885 values) and links with interference-free $PSR_i < 0.01$ (9109 values), respectively, for trials 1.34-1.52 (two transmitters, channel 14, CCA turned on). Inter-transmitter links are filtered out.

In Fig. 17, we compare the distribution of TXR differences between successive versions using box plots. Since the interquartile range would not be visible, we used the 5. and 95. percentile with the boxes. In addition, the whiskers extend to the 1. and 99. percentile, respectively. The diagram on the left side of the figure compares the versions we used in the evaluation in the previous sections. In this category, most experiments have been conducted at night on the exclusive channel 14 with CCA turned on. The diagram on the right side presents the difference distributions for experiments on channel 14 during daytime (1.57-1.59), on channel 6 during nighttime (1.60-1.62) and daytime (1.63-1.65). We refer to the former on the left side as evaluation versions, and to the latter as experimental versions. Remember that each measurement version consumed about 3 hours, and the execution order of individual experiments was fixed across all versions. Hence, we now compare two measurement values, which are separated by 3 hours.

The diagrams in Fig. 17 indicate that the majority of transmitters differ only insignificant in their TXR for the evaluation versions. In particular, 90 % of all transmitters differ by less than ± 0.03 in normalized TXR. On the non-exclusive channel 6, the variation is higher even at night, e.g. the 5.-95. percentile range is ± 0.09 for the difference between versions 1.61 and 1.62. Furthermore, the differences are higher during daytime, which is evident for versions 1.57-1.58 on channel 14 and 1.63-1.64 on channel 6. We suppose that environmental mobility is a main cause for the higher variations during daytime.

In Fig. 15, we plotted the distribution for PSR differences between successive versions. Note that the box now corresponds to the 10. and 90. percentile, respectively. The diagrams indicate that the PSR is not as stable in time as TXRs. Nevertheless, the variability is still surprisingly low. In particular, 80 % of all links vary at most by ± 0.05 , and

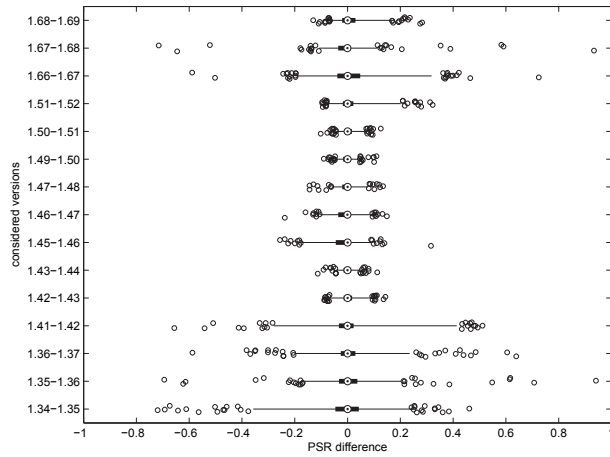
98 % are within ± 0.25 for almost all evaluation versions. Especially the first measurement versions in the evenings show the highest deviations. However, some people leave the office at that time; hence, the late-night measurements are more reliable. Furthermore, the observations about daytime and TXR hold in the same way for PSR: During daytime, the variability is higher on both channel 14 and 6. Interestingly, during the night the PSR on channel 6 is comparable stable to channel 14, e.g. the differences between version 1.61 and 1.62 are within ± 0.03 (± 0.12) for 80 % (98 %) of all links. In other words, a link can be stable even in the presence of moderate uncontrolled interference. If we consider the versions 2.10 to 2.14 in Fig. 15b, it is evident that we achieve a high stability in PSR even with heavy but controlled interference. On the other hand, the daytime variability on channel 6 is higher than on channel 14, if we compare 1.57-1.58 to 1.63-1.64 and 1.58-1.59 to 1.64-1.65. Hence, we suppose that uncontrolled interference on channel 6 during daytime contributes to this observation. Remember the campus network also uses that channel 6, which has been active during our measurements. The observations about PSR apply to RSSI, as well. However, for the sake of completeness the difference distributions are shown in Fig. 16.

IX. RELIABILITY OF RSSI ESTIMATES

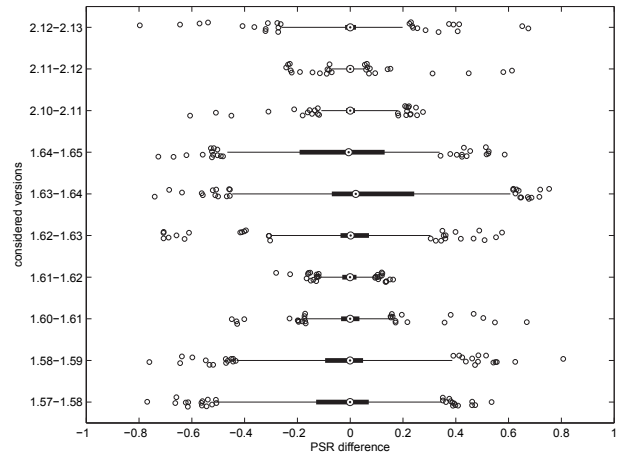
We encountered that one particular feature of the Atheros hardware may lead to complications in reproducing our results. The MadWiFi driver regularly calibrates the hardware and adapts the noise level. We noticed that after a calibration, the RSSI as reported within the AthDesc headers sometimes abruptly changed by up to 40 dB without affecting the receiver performance. This happened especially often with two transmitters and CCA turned off. After turning off the calibration, the mysterious RSSI jumps disappeared. Hence, we assume that the hardware tries to estimate a value for the noise floor during calibration, which is hardly possible if two unsynchronized senders transmit continuously. Afterwards, it reports all RSSI values in relation to the estimated noise floor. However, due to the large update interval of either 1 or 30 seconds, the dynamic noise floor estimation is too coarse to be of any value, and even worse, it causes inconsistent RSSI jumps during the measurement.

After turning off the calibration, we detected another anomaly in relation to the statistical dispersion of the RSSI during the experiments. In Fig. 18, we plotted the standard deviation in relation to the strength of both primary and secondary link. With strong primary and weak secondary links, the standard deviation seems to increase with peaks up to 10 dB, although the standard deviation of the primary links without interference is bounded by 1.5 dB with only few outliers up to 2 dB. Furthermore, we validated that the observations apply as well to other measurements with working CCA with only a slightly lower intensity.

With interference, the distribution of RSSI values becomes multimodal. Consider Fig. 19 for example, which shows the distribution of RSSI values during our experiments for several

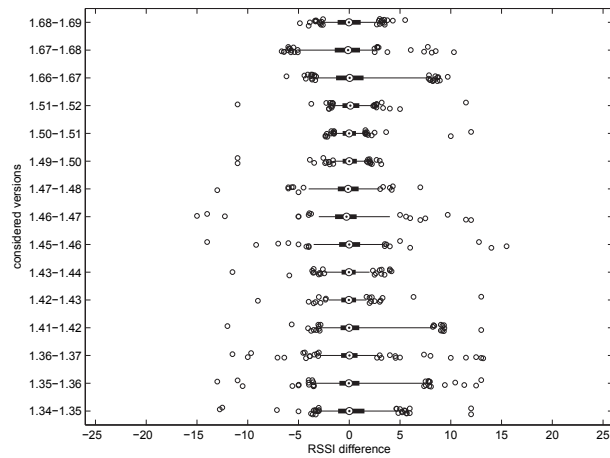


(a) Channel 14, Night, and CCA

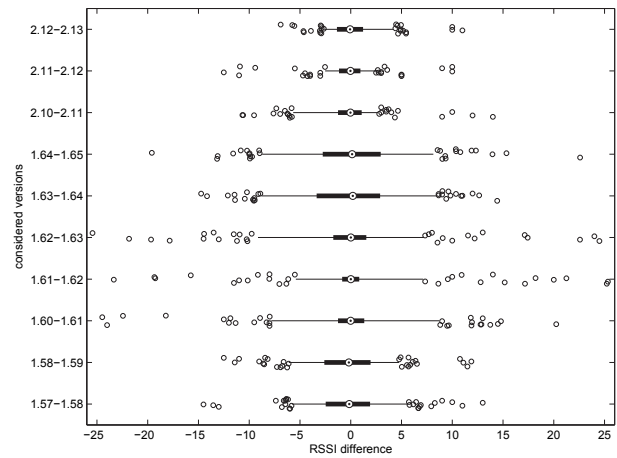


(b) Channels 6 & 14, Night & Day, CCA on & off

Fig. 15. Box plot of the distribution of PSR differences between successive versions for all experiments with either one or two senders. The box has lines at the 10. and 90. percentile, and the whiskers extend to the 1. and 99. percentile, respectively. The median is shown as a spot within the box. Data points outside of the whiskers are plotted individually.

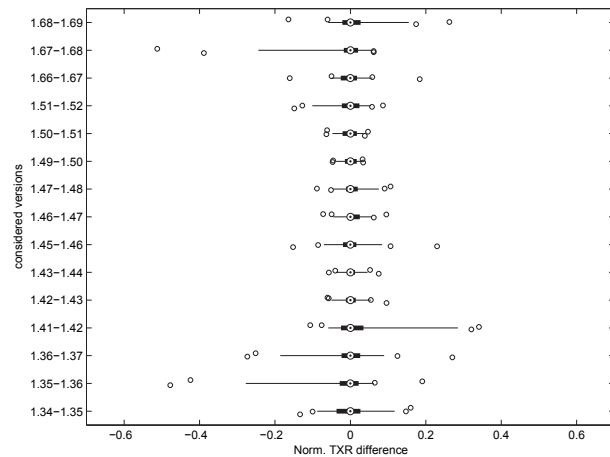


(a) Channel 14, Night, and CCA

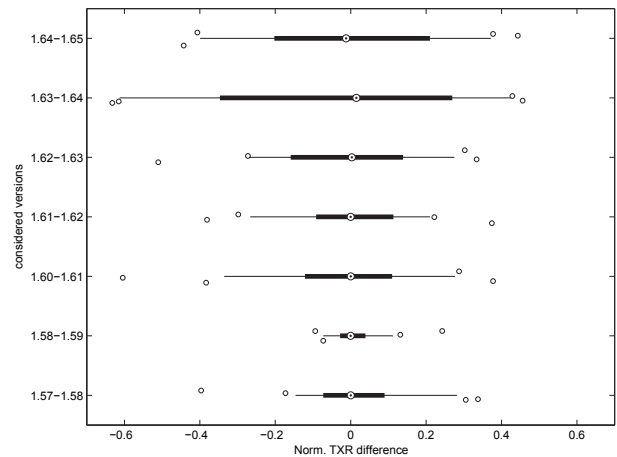


(b) Channels 6 & 14, Night & Day, CCA on & off

Fig. 16. Box plot of the distribution of RSSI differences between successive versions. The definition of the boxes corresponds to Fig. 15.



(a) Channel 14, Night, and CCA



(b) Channels 6 & 14, Night & Day, CCA on & off

Fig. 17. Box plot of the distribution of normalized TXR differences between successive versions. The definition of the boxes corresponds to Fig. 15 except that the 5. and 95. percentile is used with the boxes.

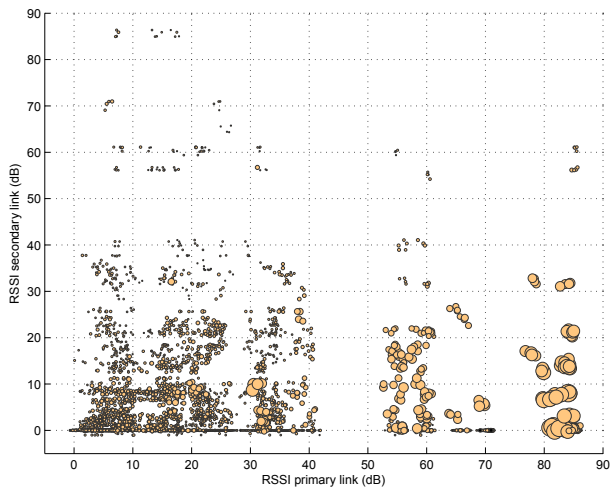


Fig. 18. Standard deviation of the RSSI values during an experiment (marker diameter) in relation to the strength of primary and secondary links with CCA turned off (trials 2.10-2.13). We filtered all links having a PSR below 0.01. Light markers represent experiments with two transmitters. For the measurements with only a single transmitter, the diagram contains dark markers on the abscissa. However, they are comparatively insignificant and thus hardly visible.

links. Without interference on link 63-31, almost all RSSI values are within 59 dB ... 62 dB. Using the additional transmitter 25, the RSSI distribution shows significant peaks around 25 dB and 50 dB. The same is observable at receiver 81 with only slightly shifted peaks. The signal strength of the secondary link is 7 dB and 14 dB at receivers 31 and 81, respectively. The RSSI drops are evenly distributed over the whole 30-second measurement duration. We furthermore noticed a weak correlation between both receivers, i.e. if one receiver experiences a low RSSI, the probability for such an event at the other receiver increases. On the other hand, both nodes are placed in neighboring rooms, thus the interference at both receivers is most likely similar. However, the observation is also present for stronger and weaker secondary links, e.g. the links 41-31 and 54-31: The strength of the former is 16 dB, and the latter is not able to deliver packets. Since the RSSI is estimated from the preamble section only [18], the results indicate that the RSSI drops relate the secondary to the primary link in terms of a repetitive relative timing. However, a detailed investigation of how it relates to physical capture and whether the receiver performance decreases is left for future work. Due to the multimodal nature of the RSSI distributions, mean and standard deviation should be handled with care unless the outlier modes have been filtered.

X. CONCLUSION

Our results show that the performance of WMNs in isolation is less random than several prior studies suggested. In particular, the performance of interference- and noise-limited receivers is different, most likely due to the capture effect. Furthermore, wireless links show a high stability in time for both receiving performance and CS. Interestingly, for IEEE 802.11b at 1Mbps, the interference and CS range

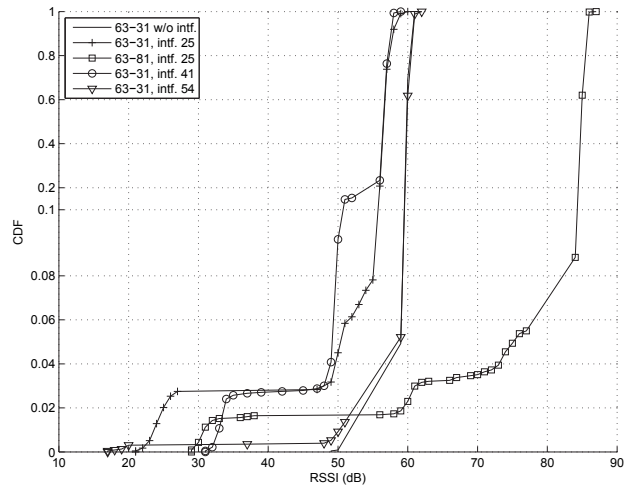


Fig. 19. CDF of RSSI values within an experiment for several links of measurement trial 2.13. Note that RSSI values, as reported by Atheros hardware, are discrete.

are only slightly larger and smaller than the receiving range, respectively. In comparison, state-of-the-art packet simulators like ns-2 and JiST/SWANS assume that the CS range is significantly larger than the receiving range. For example, the default settings of sensitivity and receiving threshold are -91 dBm versus -81 dBm for JiST/SWANS and -108.07 dBm versus -94.375 dBm for ns-2.

On the other hand, we identified uncontrolled external interference and environmental mobility as the key disturbing factors causing variations in packet reception and CS. The implications are manifold. For example, state-of-the-art simulator models of WMNs either attribute link errors to fading or use simplified synthetic loss models. However, they do not reproduce the correlation structure of external interference and environmental mobility. Furthermore, the insight about main disturbing factors in indoor WMNs should be the first step in finding new strategies to mitigate them, or even benefit from them. On the other hand, this insight is useful to eliminate approaches with little prospect of success like space-time coding, since fading is not the dominating problem in indoor WMNs.

In addition, we identified two pitfalls in obtaining accurate RSSI estimates. The dynamic noise floor adaptation present in the MadWiFi driver is not able to cope with interference, resulting in unstable RSSI values. In addition, the vendor specific estimation of RSSI is vulnerable to interference. Hence, RSSI estimates under interference have to be handled with care.

The three most important issues for our future work are as follows. We would like to investigate whether different bit-rates produce similar results, in particular when using the OFDM physical layer. Secondly, we are interested in if and how the RSSI estimation error affects the receiver performance. Furthermore, we would like to take a deeper look at the impact of multi-way interference, i.e. using more than one interfering node.

REFERENCES

- [1] D. Aguayo, J. Bicket, S. Biswas, G. Judd, and R. Morris, "Link-level measurements from an 802.11b mesh network," *SIGCOMM Comput. Commun. Rev.*, vol. 34, no. 4, pp. 121–132, October 2004.
- [2] K. Chebrolu, B. Raman, and S. Sen, "Long-distance 802.11b links: performance measurements and experience," in *MobiCom '06: Proceedings of the 12th annual international conference on Mobile computing and networking*. New York, NY, USA: ACM Press, 2006, pp. 74–85.
- [3] D. Gokhale, S. Sen, K. Chebrolu, and B. Raman, "On the feasibility of the link abstraction in (rural) mesh networks," in *INFOCOM 2008. The 27th Conference on Computer Communications. IEEE*, 2008, pp. 61–65.
- [4] J. Zhang, K. Tan, J. Zhao, H. Wu, and Y. Zhang, "A practical SNR-guided rate adaptation," in *INFOCOM 2008. The 27th Conference on Computer Communications. IEEE*, 2008, pp. 2083–2091.
- [5] J. C. Bicket, "Bit-rate selection in wireless networks," Master's thesis, Massachusetts Institute of Technology. Dept. of Electrical Engineering and Computer Science, 2005.
- [6] J. Padhye, S. Agarwal, V. N. Padmanabhan, L. Qiu, A. Rao, and B. Zill, "Estimation of link interference in static multi-hop wireless networks," in *IMC '05: Proceedings of the 5th ACM SIGCOMM conference on Internet Measurement*. Berkeley, CA, USA: USENIX Association, 2005, p. 28.
- [7] S. M. Das, D. Koutsonikolas, C. Y. Hu, and D. Peroulis, "Characterizing multi-way interference in wireless mesh networks," in *WinTECH '06: Proceedings of the 1st international workshop on Wireless network testbeds, experimental evaluation & characterization*. New York, NY, USA: ACM Press, 2006, pp. 57–64.
- [8] J. Lee, S.-J. Lee, W. Kim, D. Jo, T. Kwon, and Y. Choi, "Understanding interference and carrier sensing in wireless mesh networks," *IEEE Communications Magazine*, 2008.
- [9] J. Lee, W. Kim, S.-J. Lee, D. Jo, J. Ryu, T. Kwon, and Y. Choi, "An experimental study on the capture effect in 802.11a networks," in *WinTECH '07: Proceedings of the the second ACM international workshop on Wireless network testbeds, experimental evaluation and characterization*. New York, NY, USA: ACM, 2007, pp. 19–26.
- [10] W. Kim, J. Lee, T. Kwon, S. J. Lee, and Y. Choi, "Quantifying the interference gray zone in wireless networks: A measurement study," in *Communications, 2007. ICC '07. IEEE International Conference on*, 2007, pp. 3758–3763.
- [11] J. Lee, S.-J. Lee, W. Kim, D. Jo, T. Kwon, and Y. Choi, "RSS-based carrier sensing and interference estimation in 802.11 wireless networks," in *Sensor, Mesh and Ad Hoc Communications and Networks, 2007. SECON '07. 4th Annual IEEE Communications Society Conference on*, 2007, pp. 491–500.
- [12] C. Kai and S. C. Liew, "Towards a more accurate carrier sensing model for csma wireless networks," *CoRR*, vol. abs/0809.4342, 2008.
- [13] IEEE 802 LAN/MAN Standards Committee, "Wireless LAN Medium Access Control (MAC) and Physical Layer (PHY) Specifications. IEEE Standard 802.11," 1999.
- [14] —, "Wireless LAN Medium Access Control (MAC) and Physical Layer (PHY) specifications, Amendment 1: High-speed Physical Layer in the 5 GHz band. IEEE Standard 802.11a," 1999.
- [15] —, "Wireless LAN Medium Access Control (MAC) and Physical Layer (PHY) specifications, Amendment 4: Further Higher-Speed Physical Layer Extension in the 2.4 GHz Band. IEEE Standard 802.11g," 2003.
- [16] G. Bianchi, "Performance analysis of the ieee 802.11 distributed coordination function," *Selected Areas in Communications, IEEE Journal on*, vol. 18, no. 3, pp. 535–547, 2000.
- [17] D. S. J. De Couto, D. Aguayo, J. Bicket, and R. Morris, "A high-throughput path metric for multi-hop wireless routing," in *MobiCom '03: Proceedings of the 9th annual international conference on Mobile computing and networking*. ACM Press, 2003, pp. 134–146.
- [18] S. Leffler, "Multimode Atheros driver for WiFi on Linux," <http://www.madwifi-project.org>, 2008.